

# Numerical Investigation on Flow Structure Characteristics of Nozzle under Lower Temperature

Genzhu Jiang<sup>1,2,\*</sup>, Yulong Xie<sup>1,2</sup>, Huili Luo<sup>1,2</sup>, Minglu Dai<sup>1,2</sup>, Jigang Wang<sup>1</sup>, Xiaorong Wang<sup>1,2</sup>

<sup>1</sup>School of Mechanical Engineering, Jiangsu University of Science and Technology, Zhenjiang 212003, China

<sup>2</sup>Jiangsu Provincial Key Laboratory of Advanced Manufacturing for Marine Mechanical Equipment, Jiangsu University of Science and Technology, Zhenjiang 212003, China

\*Corresponding author

E-mail: 617352961@qq.com

## Abstract

Rocket engine is the main power unit of space transportation system and space vehicle propulsion and control. For rocket engine, nozzle is an important part that makes the rocket engine produce thrust. In this paper, the established conical nozzle model was analyzed and the flow parameters of three kinds of nozzle with straight inclination in the expansion section at three different outlet ambient temperatures were compared by using Ansys software and CFD method. Through the analysis and calculation of the data from the comparison, it is concluded that the temperature at the nozzle outlet has no influence on the velocity of flow inside the nozzle and the pressure on the wall. And there is a big difference between the outlet temperature and the temperature in the nozzle, so it has no influence on the fluid temperature in the pipe. The velocity, temperature and wall pressure of the nozzle are only affected by the inclination of the nozzle. So in  $-40^{\circ}\text{C}$  environment, nozzle can still work normally.

**Keywords:** Lavar nozzle; Conical nozzle; Low temperature; CFD.

## 1. Introduction

Nozzle is an important part of aviation propulsion system, which is widely used in various supersonic aircraft propulsion systems, such as solid rocket engine and supersonic jet engine. Its main function is to accelerate the high-temperature and high-pressure gas expansion behind the turbine and expel it from the body, so as to generate thrust of the engine. The flow characteristics of the nozzle have a great influence on the generation of thrust of the engine. The design and research of nozzle are mainly based on wind tunnel test, gas dynamics and computational fluid dynamics. Wind tunnel test cycle is long, cost is large, and there are limitations of air temperature, pressure, velocity and model size, etc. At present, computational fluid dynamics (CFD) method has become a conventional aerodynamic analysis method[1].

Lavar nozzle is a typical supersonic nozzle. The flow velocity can be controlled by changing the cross-sectional area of the pipe, which can accelerate the flow from subsonic velocity to supersonic velocity. Different nozzle models have great influence on the flow state. There are many researches on the nozzle design of rocket engine. For example, xu et al. mentioned the influence of nozzle area ratio and nozzle geometry character on the efficiency when studying rocket engine efficiency. Only when the nozzle area ratio and nozzle geometry character meet certain relationship, can the efficiency of rocket

engine be maximized[2]. The design and research of the simulation method of supersonic nozzle by computer also have obvious achievements. For example, Li Yang et al. carried out numerical simulation on the flow process of the flow field in the physical model of the axisymmetric rocket engine through Fluent software, analyzed the internal aerodynamic characteristics of the nozzle, and obtained the important characteristics of the flow field in the nozzle of the rocket engine, providing reference for the optimization design of this type of nozzle[3]. Two novel supersonic nozzles-tip ring supersonic nozzle and elliptic sharp tipped shallow lobed nozzle have been developed to enhance mixing at high speeds which is beneficial to supersonic ejectors[4]. In other areas of research, Abderrahmane Zidane et al. conducted a numerical study on the flow of the nozzle of the H<sub>2</sub>-O<sub>2</sub> rocket under chemical and vibration non-equilibrium conditions. Vibrational nonequilibrium effects on flowfield parameters and on nozzle performances are computed and shown to be minor. A reduction of 90% of computation time is observed when using the vibrational equilibrium configuration instead of the vibrational nonequilibrium configuration[5]. Bing-bing Sun et al. studied the influence of gas temperature on the damping characteristics of solid rocket engine nozzle and obtained the relationship between the cold flow coefficient and the heat transfer coefficient[6]. I.E. Ivanov carried out a numerical study on the condition of limiting shock wave separation and free shock wave separation in rocket engine thrust optimization nozzle[7]. The ablation of rocket nozzle is also studied. For example, Su Junming et al. investigated the influence of thermal environment of nozzle on the ablation rate of carbon-based throat liner[8]. A. Turchi et al. studied the gas-surface interaction of solid rocket nozzle by numerical method[9]. In the detection rocket flight height maximization of the best nozzle Mach number, Sang-hyeon Lee adopted the pseudo-analytical method to determine the optimal nozzle Mach number to maximize the flight height of the detection rocket in the standard atmosphere. The best nozzle Mach number can be predicted accurately so that the height of nozzle in burnout state or apogee can reach the maximum[10].

The above study on the nozzle does not mention whether the external temperature environment has an impact on the flow characteristics inside the nozzle. Therefore, this paper will explore the influence of outlet ambient temperature on the flow state in the nozzle. In view of this, CFD method and Fluent software were used to analyze the flow characteristics of different nozzles at three different temperatures.

## **2. Geometric model of nozzle and governing equation of flow field**

### **2.1. The geometric model**

The object of this paper is the axisymmetric conical laval nozzle, whose biggest characteristic is to facilitate the design and manufacture, and also to allow the gas to fully expand. Figure 1 is a two-dimensional geometric structure for calculation. In this study, the conical nozzle contraction section was kept the same, and the inlet and outlet diameters of the nozzle were 1.3 and 1.37 times of the throat diameter, respectively. The geometric model of the nozzle is changed by changing the straight line inclination of the expansion section (the straight line inclination is 11°, 12° and 13°, respectively). The three models were used to compare the flow states in the nozzle at different temperatures.

This study is the nozzle of the rocket engine, so the gas pressure at the entrance is 7 MPa and the temperature is 3400 K in the simulated conditions. The outlet temperatures are respectively 233 K, 293 K and 323 K. The pressure condition is one atmosphere, so as to analyze the flow state inside the nozzle.

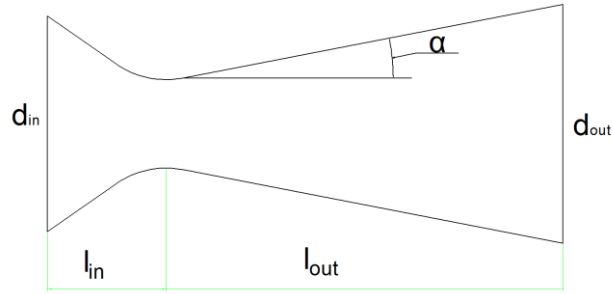


Fig.1. Schematic diagram of two-dimensional geometric structure

## 2.2. Flow field governing equation

Under the premise of ignoring the complete force, the two-dimensional axisymmetric, unsteady and compressible fluid turbulent flow Reynolds average n-s equation and the component diffusion equation are transformed as follows:

$$\frac{\partial \tilde{U}}{\partial t} + \frac{\partial \tilde{F}}{\partial a} + \frac{\partial \tilde{G}}{\partial Z} = \frac{\partial \tilde{F}_v}{\partial a} + \frac{\partial \tilde{G}_v}{\partial Z} + \tilde{S} \quad (1)$$

The flow of ideal gas in the nozzle follows the conservation of mass, momentum and energy, and the governing equations are as follows:

$$\frac{\partial \rho_v}{\partial t} + \frac{\partial}{\partial x_i} (\rho_v u_i) = 0 \quad (2)$$

$$\frac{\partial}{\partial t} (\rho_v u_i) + \frac{\partial}{\partial x_j} (\rho_v u_j u_i) = -\frac{\partial p}{\partial x_i} + \frac{\partial}{\partial x_j} \left[ u \left( \frac{\partial u_j}{\partial x_i} + \frac{\partial u_i}{\partial x_j} - \frac{2}{3} \delta_{ij} \frac{\partial u_l}{\partial x_l} \right) \right] + \frac{\partial}{\partial x_j} (-\rho_v \overline{u_i u_j}) \quad (3)$$

$$\frac{\partial}{\partial t} (\rho_v E) + \frac{\partial}{\partial x_j} (\rho_v u_j E + u_j p) = \frac{\partial}{\partial x_j} (k_{eff} \frac{\partial T}{\partial x_j} + u_i \tau_{eff}) \quad (4)$$

where:  $\rho_v$  is gas density;  $u_i$  and  $u_j$  are the velocity component;  $p$  As the pressure;  $T$  is the temperature;  $\mu$  As the viscosity;  $\delta_{ij}$  is the Kronecker delta number;  $E$  is the total energy of the gas;  $k_{eff}$  is effective thermal conductivity;  $\tau_{eff}$  is the effective stress tensor.

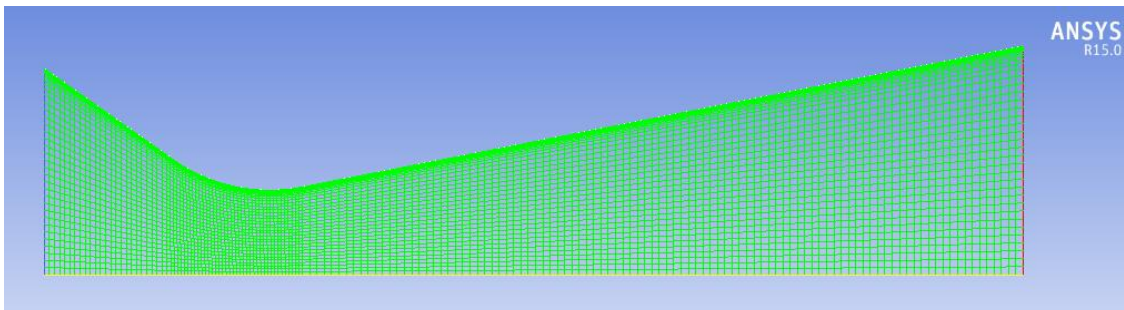


Fig.2 Meshing diagram of the conical nozzle

## 3. The Grid division of nozzle and CFD calculation method

### 3.1. Grid division of physical model of conical nozzle

This model adopts the method of subregional grid and carries out regional division for the convenience of grid division. The model is divided into three parts. The structured grid is used to divide the boundary layer, and the boundary layer is locally encrypted considering the influence of the boundary layer. Because the throat calculation is complex, so the throat of the nozzle is also encrypted. The total number of grids is 12,435. The divided grid model is shown in Fig. 2.

### 3.2. Determination of calculation model and solution method

(1) Because of the compressible nature of the medium on the rocket nozzle, the RNG k- $\epsilon$  model is suitable. RNG K- $\epsilon$  is more accurate than the standard K- $\epsilon$  model. Considering the eddy generation by turbulence, the RNG K- $\epsilon$  model is adopted.

(2) The gas flow in the nozzle belongs to the high-speed compressible flow, which can be solved by using the density basis method.

(3) To improve the overall calculation accuracy. The flow governing equation, turbulent kinetic energy equation and turbulent dissipation rate equation were discretized by the second-order windward scheme.

### 3.3. Determination of boundary conditions

For the boundary conditions, the nozzle inlet is set as the mass flow rate inlet, the mass flow rate is 18 kg/s, and the inlet pressure is 7 MPa. The outlet is set as pressure outlet is 0.1 MPa, and the solid wall is set as no slip, no seepage and adiabatic boundary. The mass flow rate inlet specifies the surface pressure, total temperature and turbulence parameters. For supersonic flows, since all flow parameters will be derived from the interior, the pressure outlet is not set accordingly. In case of changing the back pressure, the pressure outlet specifies static pressure, total reflux temperature and turbulence parameters. The boundary conditions of the nozzle are shown in Fig. 2.

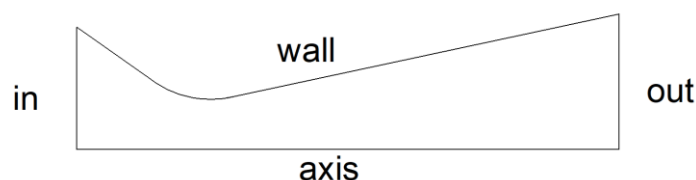


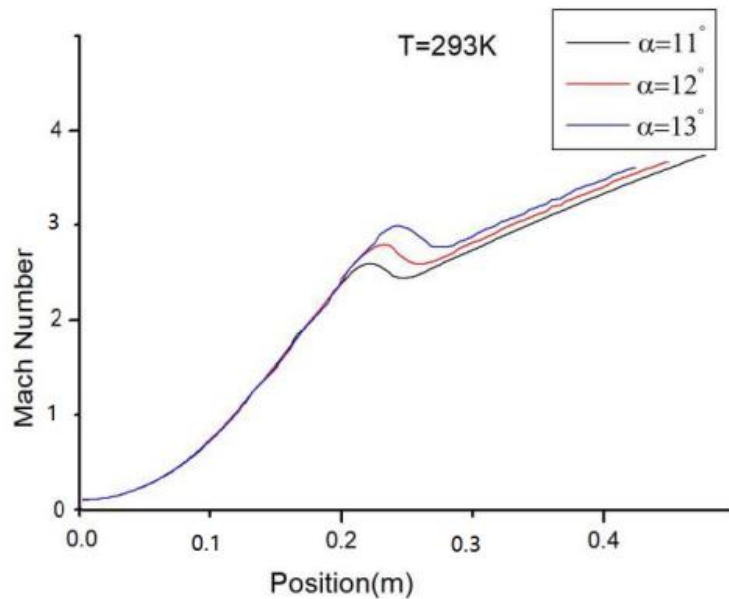
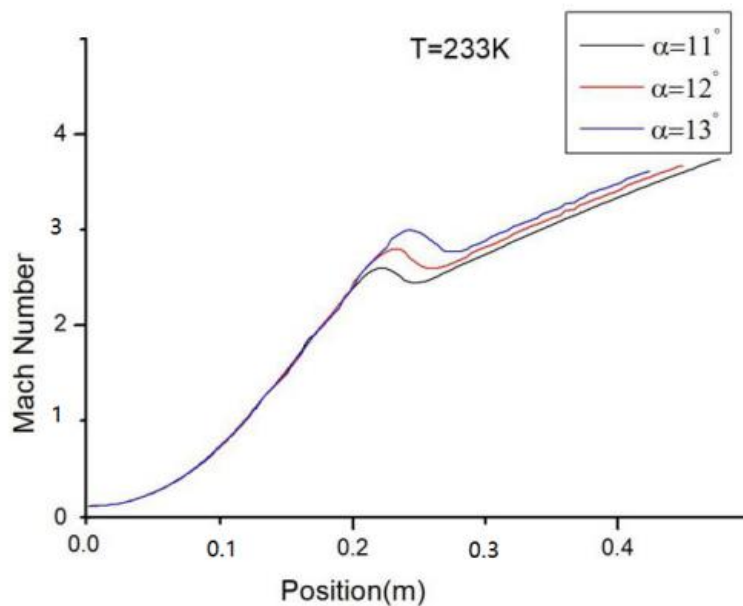
Fig.3 Boundary conditions of the nozzle

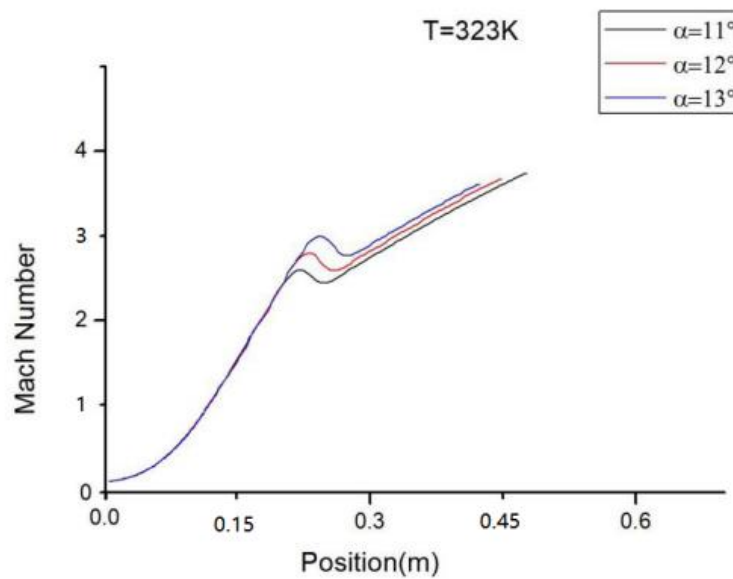
## 4. Analysis of calculation results

### 4.1. Mach number analysis

Fig. 4 show the comparison of axial Mach number curves of nozzles with different inclinations at 293 K, 233 K and 323 K, respectively. Fig. 5 is a comparison diagram of the axial Mach number curves of the nozzle with a dip Angle of  $11^\circ$  at 293 K, 233 K and 323 K temperatures. Fig. 5 shows the trend of Mach number along the axis and the Mach number cloud diagram. The figure shows that temperature has little effect on the Mach number. The maximum Mach number difference value between the minimum temperature and the maximum temperature is 0.0015. Fig. 4 show that the influence of velocity change is the magnitude of the inclination of the straight line in the expansion section of the nozzle. The three models have the same trend of Mach number change from inlet to throat. Mach number is one at the throat. At approximately 0.17 m from the nozzle inlet, the Mach number begins to decrease. The reason is that the wall slope suddenly increases due to the dip Angle at the throat outlet, and the direction change

becomes more prominent for the fluid, so the fluid cannot flow close to the wall surface, and the shock wave is formed. So there was a loss of thrust. When we get through this phase, the fluid flows close to the wall, and the airflow velocity increases gradually. Moreover, about 0.17 m away from the nozzle inlet, the velocity inside the nozzle with a large inclination of the model began to change, and the velocity with a large inclination of the nozzle was greater than the velocity with a small inclination of the nozzle. The Mach number of the nozzle with an expansion angle of  $11^\circ$  at the outlet of the nozzle was higher than that of the other two nozzles, reaching 3.74, while maintaining the same diameter of the outlet of the expansion section.

(a)  $T=293\text{ K}$ (b)  $T=233\text{ K}$



(c) T=323 K

Fig. 4 At 293 K, 233 K and 323 K respectively, the trend of Mach number along the axis with three different expansion angles nozzle

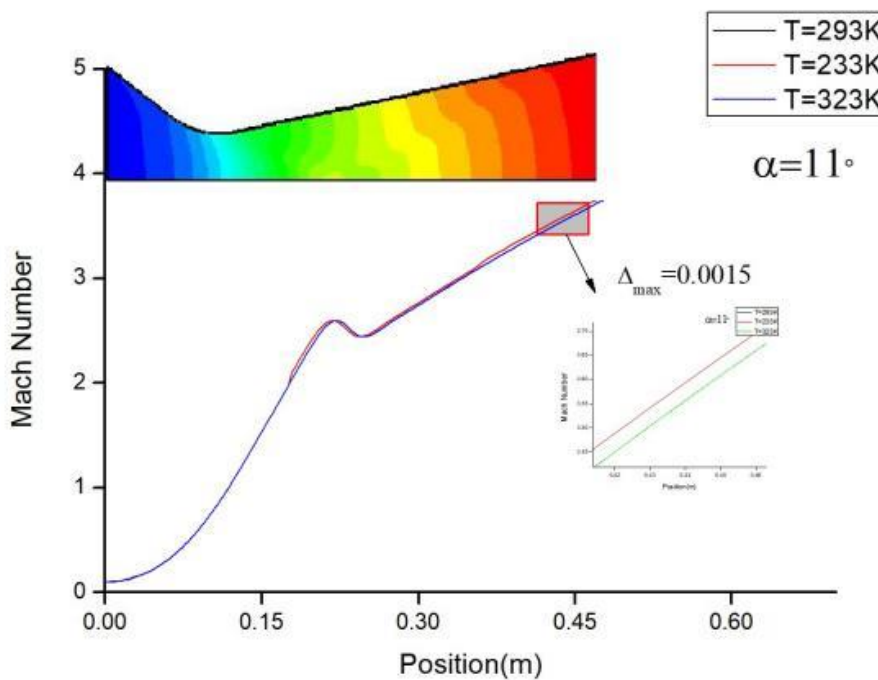
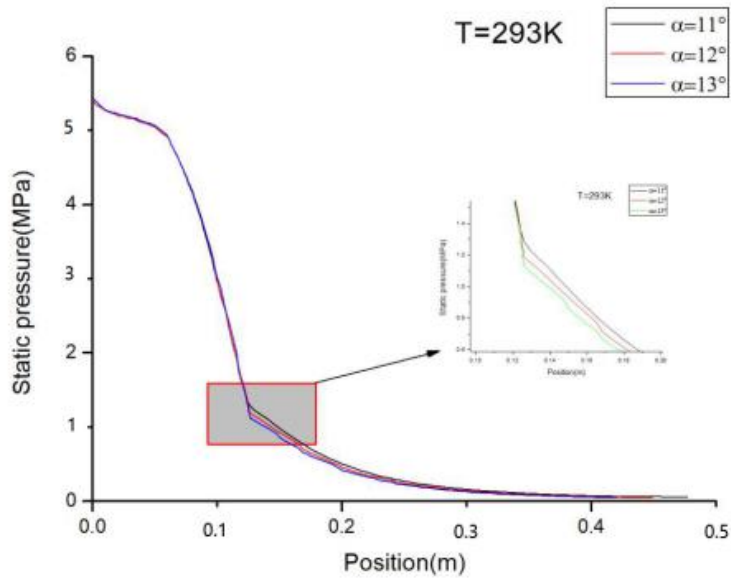


Fig.5 The trend of Mach number along the axis under three temperature conditions

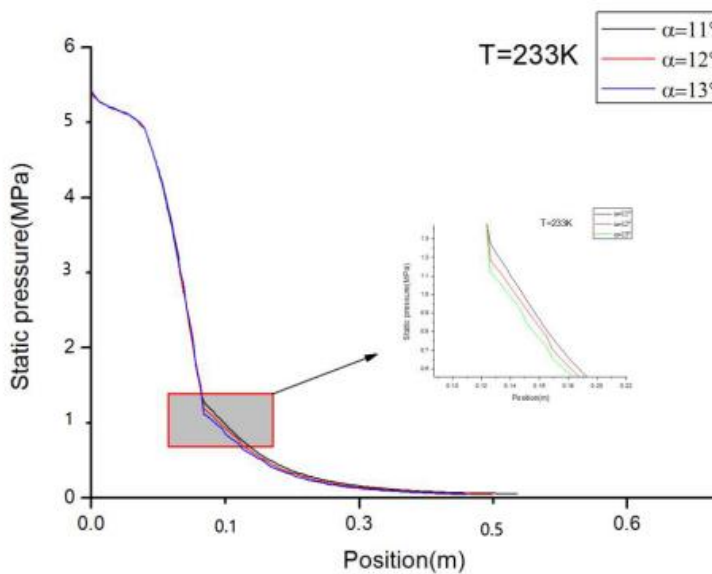
#### 4.2. Comparative analysis of pressure

Fig. 6 is a pressure on wall curve along the axis at three different temperature. It can be seen that the overall pressure trend of three conical angle nozzles in different expansion sections is similar. And it can be seen from Fig. 7 that the outlet temperature of the nozzle has almost no effect on the pressure inside

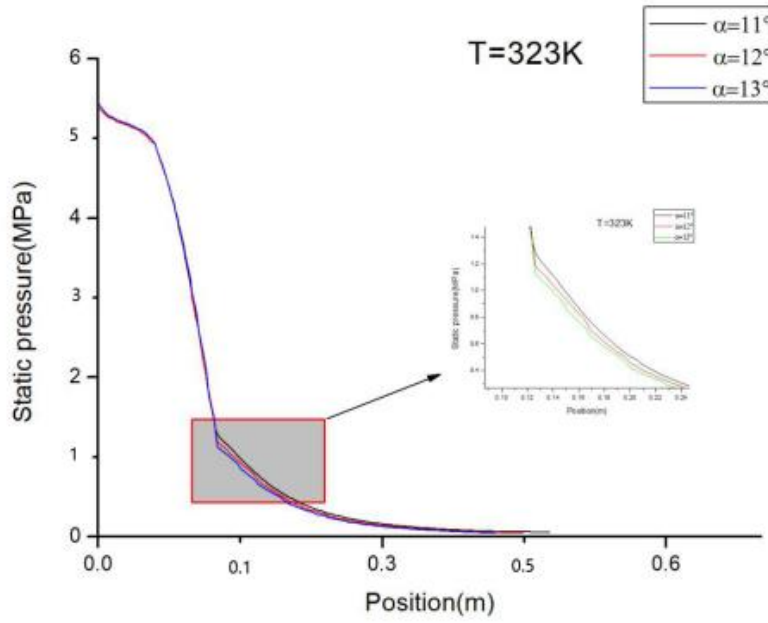
the nozzle. As shown in the figure, the wall pressure along the axis of laval nozzle changes dramatically in the contraction section and throat position. That is, 0.05-0.14 m of the nozzle. So in this section of the application of higher strength of protective materials. The pressure on the wall of the expansion section decreases slowly. According to the enlarged drawing of the red box in the figure, the pressure at the throat outlet of the nozzle with a expansion Angle of  $11^\circ$  is slightly higher than that inside the other two nozzles. The pressure on the inner wall of the nozzle decreases with the linear inclination angle increasing. This is because the nozzle contraction section is the same, before the throat wall pressure is the same. At the time of reaching the expansion section, the wall surface of the nozzle with a large inclination has a small component force due to the different inclination Angle of the expansion section. The wall pressures of the three nozzles at the end of the nozzle gradually become the same.



(a) T=293 K



(b) T=233 K



(c) T=323 K

Fig. 6 At 293 K, 233 K and 323 K respectively, the trend of pressure on wall along the axis with three different expansion angles nozzle

In order to make the nozzle flow free from external interference,  $p_e > p_a$  must be satisfied, which is the mechanical condition of nozzle design. The pressure of all three nozzles was reduced to 0.1 MPa at 0.37 m. The flow in the nozzle is disturbed from the outside. Therefore, it is necessary to appropriately increase the inlet pressure to make the outlet pressure  $p_e > p_a$ .

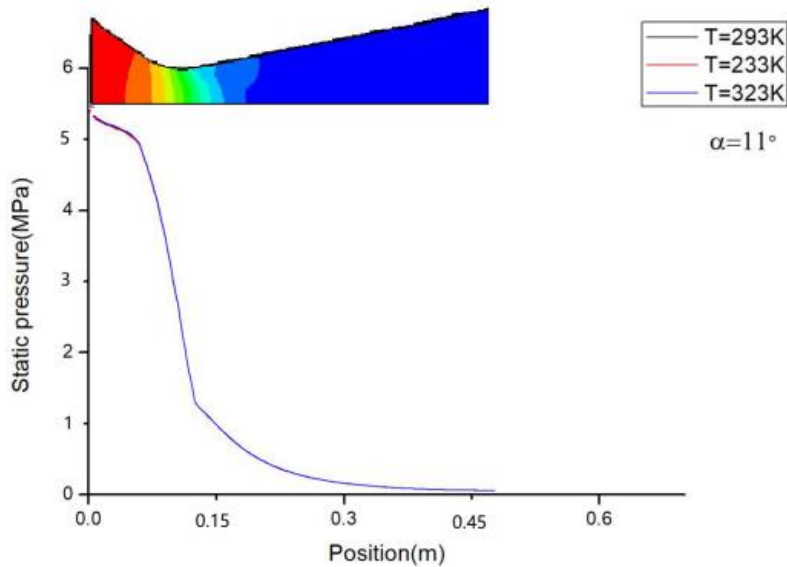


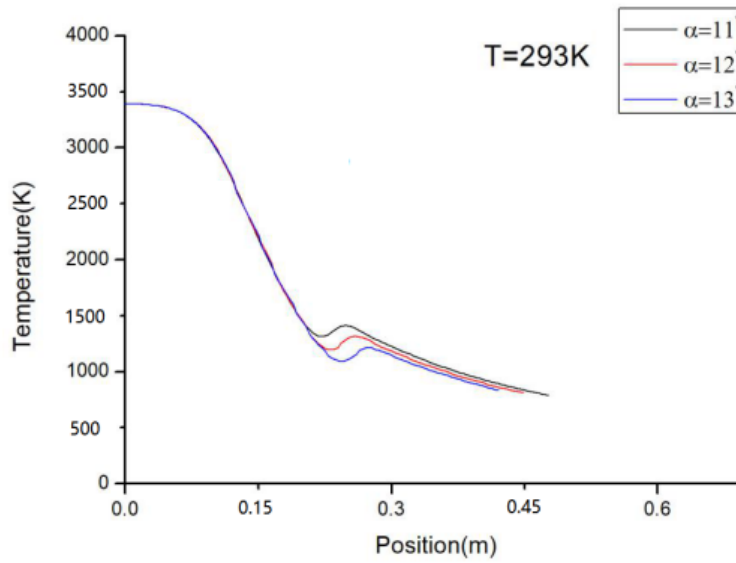
Fig.7 The trend of pressure on the wall along the axis under three temperature conditions

#### 4.3. Axial temperature analysis

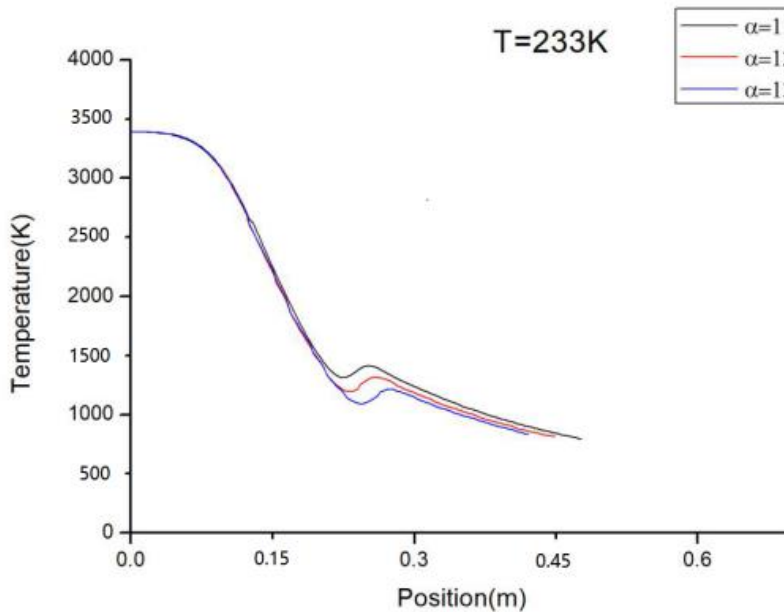
Fig. 8 shows that the inlet temperature of the nozzle is selected as 3400 K, and the gas flows in the



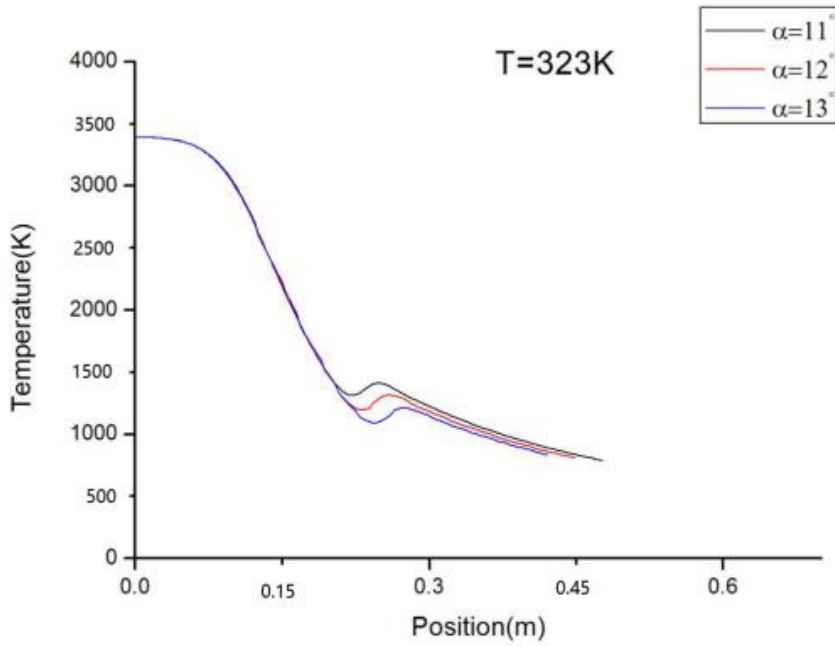
nozzle, and the temperature keeps decreasing. Among them, the temperature in laval nozzle changes sharply in the contraction section and throat position. Ablative materials should be selected in this section. After that, the temperature in the expansion section fluctuates, and the temperature curves of three different inclination nozzles at this position are different. The nozzle with an expansion angle of  $11^\circ$  had the highest temperature, and the nozzle with an inclination angle of  $13^\circ$  had the lowest temperature. Fig. 9 is the trend of temperature along the axis under three temperature conditions and temperature nephogram and shows that maximum temperature difference between nozzles is 54.23 K. Because the temperature at the outlet is quite different from that in the pipe, it has no influence on the gas temperature in the pipe.



(a) T=293 K



(b) T=233 K



(c)  $T=323\text{ K}$

Fig. 8 At 293K, 233K and 323K respectively, the trend of temperature along the axis with three different expansion angles nozzle

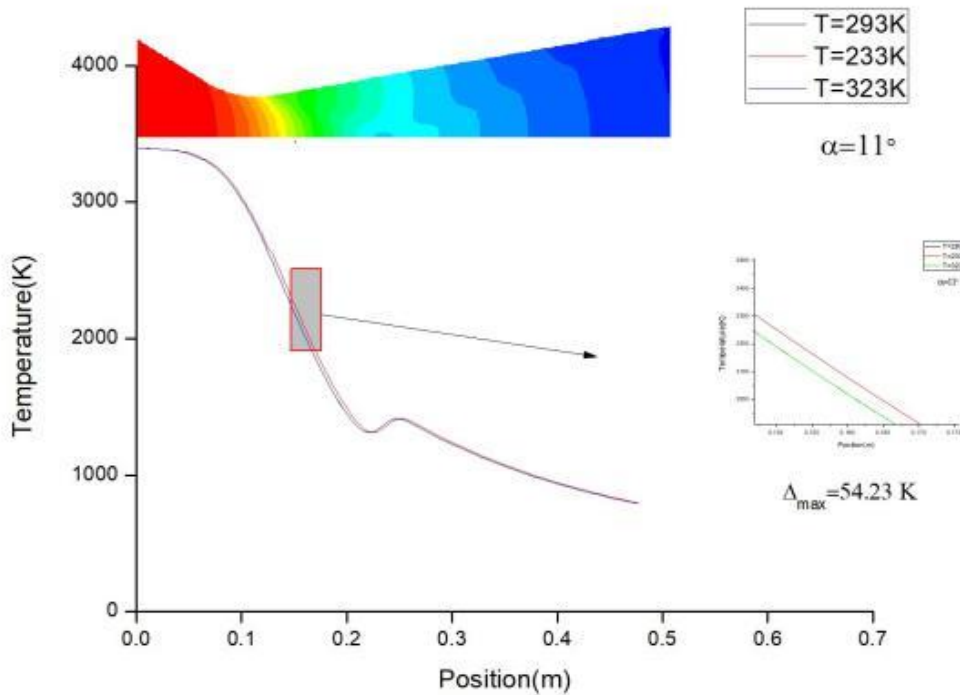


Fig.9 The trend of temperature along the axis under three temperature conditions

**5. Conclusion**

- (1) The temperature change at the nozzle outlet has almost no influence on the gas velocity, pressure

and temperature inside the nozzle. So the nozzle can work normally in some cold places.

(2) The linear inclination of the nozzle expansion section is the key factor affecting the flow state of the fluid inside the nozzle. The greater the inclination, the lower the velocity of the nozzle at the same axis. On the contrary, for the influence of pressure and temperature, the higher the inclination angle is, the lower the wall pressure and temperature are at the same axis.

(3) The pressure and temperature of the nozzle at the contraction section and throat position change dramatically, so high protection and ablation-resistant materials should be selected.

## References

- [1] Wang Ping, Liu Xue-shan, Qiao li-min, Axisymmetric Laval nozzle flow field analysis. *Aircraft Design*, 2013, 33 (2) : 24-26
- [2] Xu Jun-min, Huang Chong-xi. Effect of rocket design parameters on the efficiency of engine nozzle. *Journal of Rocket Propulsion*, 1995, 13 (2) : 2
- [3] Li Yang, Zhang Guo-wei, Zhang Guo-dong, Numerical simulation of rocket engine nozzle flow field based on Fluent. *Electromechanical technology*, 2013, 12 (3) : 13-15
- [4] Srisha M.V. Rao a, G. Jagadeesh, Novel supersonic nozzles for mixing enhancement in supersonic ejectors. *Applied Thermal Engineering*, 2014, (71): 62-71
- [5] Abderrahmane Zidane, Rabah Haoui, Mohamed Sellam, Zineddine Bouyahiaoui, Numerical study of a nonequilibrium H<sub>2</sub>-O<sub>2</sub> rocket nozzle flow. *International journal of hydrogen energy*, 2019, (44) : 4361-4373
- [6] Sun Bing-bing, LI Shi-peng, Sun Wan-xing, Li Jun-wei, Wang Ning-fei, Effects of gas temperature on nozzle damping experiments on cold-flow rocket motors. *Acta Astronautica*, 2016, (126) : 18-26
- [7] I.E. Ivanovb, I.A. Kryukov, Numerical study of ways to prevent side loads in an over-expanded rocket nozzles during the launch stage[J]. *Acta Astronautica*, 2019
- [8] Su Jun-ming, Zhou Shao-jian, Xue Ning-juan, Xiao Chun, Effect of nozzle thermal environment on the ablation rate of the throat inserts of solid rocket motors. *New Carbon materials*, 2018, (5) : 33
- [9] A.Turchi, D.Bianchi, F.Nasuti, M.Onofri, A numerical approach for the study of the gas-surface interaction in carbon-phenolic solid rocket nozzles. *Aerospace Science and Technology*, 2013, (27) : 25-31
- [10] Sang-Hyeon Lee, Optimal nozzle Mach number for maximizing altitude of sounding rocket. *Aerospace Science and Technology*, 2018, (74) : 104-111